La mer 34: 199–214, 1996
Société franco-japonaise d'océanographie, Tokyo

Numericaling modelling on atmospheric circulations over the eastern mountainous coastal seas of Korea

Hyo CHOI*

Abstract: By one way double-nested non-hydrostatic numerical model, wind fields in the high mountainous coastal region of Korea were three-dimensionally simulated from March 27 to March 28, 1994. Strong synoptic scale westerly winds blowing over the large steep mountains in the coastal region caused localized downslope wind storms and enhanced development of easterward internal gravity waves in the lee-side of mountain.

During the day a meso scale sea breeze circulation induced by thermal forcing due to temeprature contrast of air over between land and sea progresses from sea toward inland. But it is impeded by eastward propagation of internal gravity waves and confines to the offshore side of the coast. Thus, two kinds of atmospheric circulations consist of an interna gravity wave circulation (westerly) and a sea breeze circulation (both easterly near the sea surface and westerly in the upper level). Air in the lowest atmospheric layer at Kangnung coastal site should be trapped by two opposite circulations and surface winds near the coastal seas are relatively weaker than those in the open sea or the inland sites, even if the upper level wind speeds were very strong. On the other hand, a nighttime land breeze from the inland toward the coastal sea could enhance development of existed eastward downslope wind storm and downward transport of momentum from the upper atmosphere toward the coastal surface due to disappearance of vertical thermal convection also makes a contribution to more intensification of westerly winds in the coastal region, increasing the surface wind speeds. Consequently, under the severe downslope wind storms induced by strong synoptic scale winds over the mountain toward the coastal sea, the surface wind speeds became much higher at night than in the daytime and caused much unstable sea states generated by the strong surface winds.

1. Introduction

In recent years, DURRAN and KLEMP (1987), KLEMP and DURRAN (1983), PELTIER and CLARK (1979) made numerical simulations on downslope winds, lee-side waves and up-stream blocking resulted from orographic effects in the inland mountain region. BOER *et al.* (1984), DAVIS (1987), LILLY *et al.* (1982), PALMER *et al.* (1986), SMITH (1978, 1989) and WMO (1986) carried out the thoretical and numerical studies on the surface pressure drag and wave momentum flux in the mountain ranges.

RAYNOR *et al.* (1979) and SETHURAMAN (1982) described boundary wind structure near land-sea interface and MCPHERSON (1970) mentioned distortion of sea breze convergence zone from the simulation of Galveston Bay in Texas due to the effect of irregularly shaped coastlines on predicted wind fields. SEGAL *et al.* (1982) identified calm wind zones in conjunction with sea breeze convergence front formed between nearly parallel coastlines through a three-dimensional simulation of sea breeze circulation. LANGLAND *et al.* (1987) demonstrated the result of numerical simulation on a satellite-observed calm zone over the curved coastline of Monterey Bay by using a meso scale marine boundary layer model, which is no-hydrostatic and anelastic without considering the effects of complex terrain.

In the mountainous coastal region, it is known that the patterns of atmospheric circulations are very complicated and are still unsolved problem (CHOI and CHOI, 1994; CHOI and CHOI, 1995; FRIEHE and WINANT, 1982; HSU, 1980, 1988; PLATE, 1971; SATOMURA and

* Dept artment of Atmospheric Sciences, Kangnung National University, Kangnung, Kangwondo, 210-702 korea

BOUGEAULT, 1992; SETHRAMAN, 1982). Along the coastal sea with high and steep mountains atmospheric circulations, which make a great influence upon waves and circulations, should be affected by sea-land breeze circulation and propagation of internal gravity waves in the lee-side of mountain (CHOI *et al.*, 1996; LEE, 1982; SMITH, 1989; SMOLARKIEWICZ and ROTUNNO, 1989)

In spring we often find that synoptic scale westerly winds with high wind speeds prevailed in north-eastern Asia and become enforced localized wind storms by Taegwallyang mountain near Kangnung city in the eastern coastal edge of Korea. When internal gravity waves with hydraulic jump motions, under downslope wind storms are rapidly developed in the lee-side of the coastal mountain, unusual high winds should be generated over coastal seas and resulted in high sea waves.

The purpose of this study is to explain atmospheic circulatins by using a three-dimensional numerical model, which will have a great influence upon the formation of wind driven currents and wind waves and to find out mountain effects on forecasting coastal wind fields and sea states, when both downslope wind storms and sea breeze process exist.

2. Numerical method and data analysis

As shown in Fig. 1 and 2, the study area is located in the eastern coastal region of korea (adjacent to Japan sea) with high and steep mountains, which lies from south to north parallel to coastal lines and consists of a complex terrain with sand, soil and forest in a high mountain called Mt. Taegwallyang near Mt. Whangbyung (1407m) (CHOI and CHOI, 1995). For investigating atmospheric circula-tions due to the rapid development of violent internal gravity waves and sea-land breeze circulation in Kangnung coastal region from March 26 through 29, 1994, a non-hydrostatic grid point model was adopted with some modification and one way double-nesting technique was used for precise simulation on coastal wind aspects.

We chose horizontal resolutions of the model as 20km in the coarse-mesh model and 7km in the fine-mesh for double nesting with the number of 34 × 34 grids. This model consists of 15 vertical levels from 10m to 6km over the ground such as 10, 45, 120, 235, 350, 500, 700, 900, 1100, 1400, 1800, 2400, 3200, 4200 and 5400m in z^* coordinate called a complex terrain-following coordinate, and the lowest model level is set at 10m, representing the depth of the surface layer.

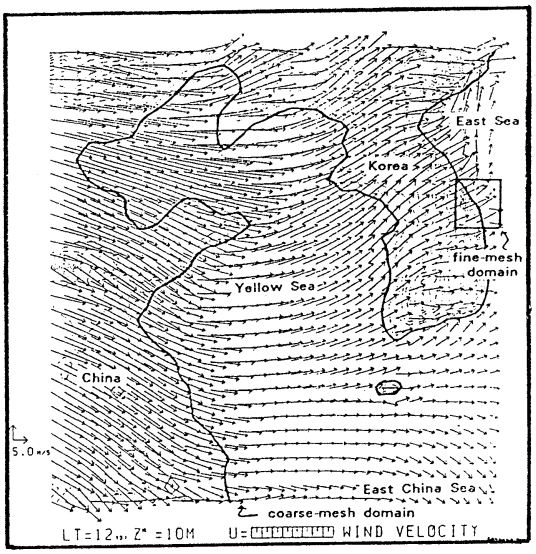

Fig. 1. Calculated wind sppeds (m/s) at 10m height over the ground surrounding the Korean peninsula at 12 LST, march 27, 1994 in the coarse domain by using Global Analysis Data.

In the coarse-mesh model, 12 hourly G-ANL (global analysis) data reanalyzed by Japan Meteorological Agency (JMA) are provided as initial data for lateral boundary of the model domain. The coarse-mesh model calculates meteorological variables at each grid point and predicted values on each variable were used again as lateral boundary data in the fine-mesh model. Through horizontal and vertical interpolations of the same global analysis data such as winds, potential temperature, specific humidity, modified data are provided as initial fields for all two models with different resolutions in this work. During the model experiment we found that horizontal gradient of sea surface temperatures on the coastal sea could also much affect the generation of coastal thermal winds comparable to horizontal gradient

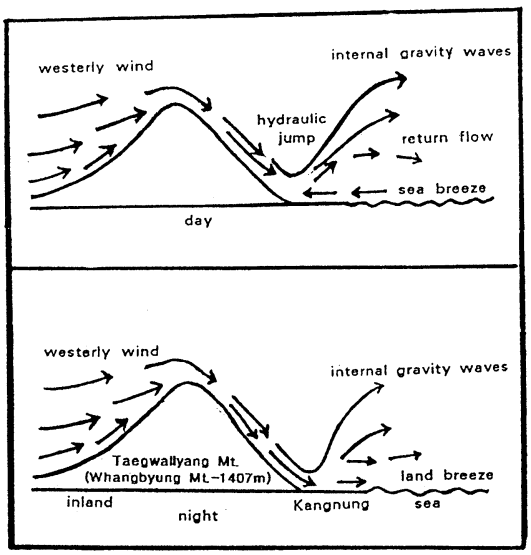

Fig. 2. Schematic profiles of air flows over the eastern mountainous coastal regions for day and night.

of air temperatures over land and sea surfaces. In order to consider effects of sea surface temperature on the coastal winds, initial temperatures of sea surface water were obtained from sea surface temperature data acquired by NOAA (National Oceanic Atmospheric Administration) satellite, which were analyzed by National Fisheries Research and Development Agency of Korea (CHOI and CHOI, 1995; 1995; NFRDA, 1994; ROLL, 1965).

A 30 hour numerical prediction experiment was carried out from an initial time, 09 LST (Local Standard Time=9h + Greenwith Mean Time), March 27 to the next day at 12 LST, March 28 by using HITACH super computer establishied at Meteorological Research Institute, JMA. After completing our numerical simulation for forecasting winds fields over the mountainous coastal seas, the simulated winds under the strong downslope wind storms were compared with observation ones measured by a pival balloon launched from Korean Air Force Base of Kangnung city at 09 LST, every day from March 27 through 29, 1994.

3. Numerical model

a. Governing equations

In the model formulae, the governing equations consist of a terrain-following coordinate system called z^* coordinate with the assumption of Boussinesq and anelastic approximations (KIMURA, 1983 and KIMURA and TAKAHASHI, 1991). For the generalized vertical coordinate transformation (x, y, z^*) from the cartesian svstem (x, v, z), the equations of motion can be derived as

$$d_t hu = fhv - h\Theta\partial_x \Pi + \Theta(z_T - z^*)\partial_x z_G \partial_z \Pi + z_T^2/h\,\partial_z(K_m \partial_z u) \quad (1)$$

$$d_t hu = -fhv - h\Theta\partial_y \Pi + \Theta(z_T - z^*)\partial_y z_G \partial_z \Pi + z_T^2 h\,\partial_z(K_m \partial_z v) \quad (2)$$

$$d_t hw^* = -z_T \Theta\,\partial_z \Pi + gh\,\theta/\Theta \quad (3)$$

and

$$\Pi = (P/P_{00})^{R/C_p}$$
$$\Theta = T(P/P_{00})^{R_d/C_p}$$
$$z^* = z_T(z - z_G)/h \quad (4)$$
$$h = z_T - z_G$$
$$d_t = \partial_t + u\partial_x + v\partial_y + w^*\partial_z$$
$$hw^* = z_T w + (z^* - z_T)(\partial_x z_G u + \partial_y z_G v)$$

Here, u, v and w^* are velocity compoments in the x, y and z directions in the z^* coordinate and g is gravity (m/s^2). Θ, T, z, z_T, z_G and K_m are potential temperature (K), air temperature at a given height, actual height, height of upper boundary with its change for time and place in a model domein, height of topography and vertical diffusion coefficient for momentum (m^2/s), respectively. P, P_{00}, R, R_d and C_p are atmospheric pressure, atmospheric pressure at reference level, universal gas constant, gas constant for dry air and specific heat at constant pressure.

The first terms on the right hand side of eqs. (1) and (2) are Coriolis forces (f; Coriolis parameter, $f=2\Omega\sin\phi$, Ω ; angular velocity of the earth rotation, ϕ ; latitude), and the second, third and fourth terms are pressure gradient forces, adjusted terms on topography and vertical diffusion. The second and third terms of eq. (3) present vertical pressure gradient force and buoyancy.

Considering the thermodynamic equation and conservation of water vapor following equations are given by

$$d_t h\Theta = z_T^2/h\,\partial_z(K_h \partial_z \Theta) + hQ_r \quad (5)$$

$$d_t hq = z_T^2/h\,\partial_z(K_h \partial_z q) \quad (6)$$

where Q_r and q are Newtonian cooling due to long wave radiation and specific humidity of water vapor. Thus, the second term of eq. (5) implies radiative heating process. For the simplicity of our model, condensation processes such as microphysics of water are not considered. The continuity equation yields to

$$\partial_x hu + \partial_y hv + \partial_z hw^* = 0 \tag{7}$$

Euler-backward scheme is adopted for the time integration of eqs. (1), (2), (5), and (6) and for the vertical direction Crank-Nicholson scheme, respectively. z_G and z_T mean the ground surface level and top boundary level with a material surface in the model atmosphere (6000m), which can absorb gravity-wave energy generated in the lower layers and the radiation condition suggested by KLEMP and DURREN (1983) was adopted for upper boundary condition.

In general, horizontal scale of the phenomena is one order greater than vertical scale, and eq. (3) can be converted into the following equation for hydrostatic equilibrium as

$$\partial_z \Pi = h/z_T \cdot g/\Theta^2 \cdot \theta \tag{8}$$

Considering that the hydrostatic equilibrium can not exist, the pressure equation for non-hydrostatic state can be given by

$$\begin{aligned}&\partial_{xx}\Pi + \partial_{yy}\Pi + \{(z_T/(z_T - z_G))^2 \\ &+ ((z^* - z_T)/h)^2((\partial_x z_G)^2 + (\partial_y z_G)^2)\}\partial_{zz}\Pi \\ &+ 2(z^* - z_T/h\partial_x z_G \partial_{xz}\Pi + 2(z^* - z_T)/h\partial_y z_G \partial_{yz}\Pi \\ &+ \{(z^* - z_T)/h(\partial_{xx} z_G + \partial_{yy} z_G) \\ &+ 2(z^* - z_T)/h^2((\partial_x z_G)^2 + (\partial_y z_G)^2)\}\partial_z \Pi \\ &= r(x,y,z^*)/(\Theta h)\end{aligned} \tag{9}$$

where r is the residual term and

$$\Pi = \pi - \pi_H \tag{10}$$

$$\partial_z \pi_H = gh\theta/(\Theta^2 z_T) \tag{11}$$

$$\begin{aligned}r(x,y,z^*) &= \partial_x ADVX + \partial_y ADVY \\ &+ z_T/h\partial_z ADVZ + 1/h\ \partial_x z_G \partial_z (z^* - z_T) ADVX \\ &+ 1/h\ \partial_y z_G \partial_z (z^* - z_T) ADVY\end{aligned} \tag{12}$$

and

$$\begin{aligned}ADVX &= -\partial_x huu - \partial_y huv - \partial_z huw^* \\ &+ fhv - \Theta h\partial_x \pi_H - \Theta(z^* - z_T)\partial_x z_G \partial_z \pi_H \\ &+ z_T^2/h\ \partial_z(K_m \partial_z u) \\ ADVY &= -\partial_x huv - \partial_y hvv - \partial_z hvw^* - fhu \\ &- \Theta h\partial_y \pi_H - \Theta(z^* - z_T)\partial_y z_G \partial_z \pi_H \\ &+ z_T^2/h\ \partial_z(K_m \partial_z v) \\ ADVZ &= -\partial_x huw - \partial_y hvw - \partial_z hww^*\end{aligned} \tag{13}$$

In the simulation processes of the model, the open boundary condition developed by ORLANSKI (1976) for u, v, θ and q was modified for the lateral boundary condition of the model domain.

b. Model formula in turbulent process

As suggested by YAMADA (1983) in the surface boundary layer the turbulent closure level-2 model is adopted for calculating turbulent diffusion coeficients, K_m and K_h for momentum and heat of eq.(1) through eq. (6) by

$$\begin{aligned}K_m &= S_m \cdot e \cdot \ell \\ K_h &= S_h \cdot e \cdot \ell\end{aligned} \tag{14}$$

where ℓ and e^2 imply turbulent length determined by diagnostic approaches and turbulent kinetic energy (m^2/s^2) as

$$\begin{aligned}\ell &= kz/(1 + \ell_0/kz) \\ \ell_0 &= 0.1\int ez\, dz/\int ez\end{aligned} \tag{15}$$

and the semi-empirical formulae between S_m S_h and flux Richardson number, R_f in the surface boundary layer can be also evaluated by

$$\begin{aligned}S_m &= 1.76\ (0.1912 - R_f)\ (0.2341 - R_f)/ \\ &\quad \{(1 - R_f)\ (0.2231 - R_f)\} = 0.085 \\ &\qquad \text{for } R_f \geq 0.16 \\ S_h &= 1.318\ (0.2231 - R_f)/(0.2341 - R_f) S_m \\ &= 0.095 \qquad \text{for } R_f \geq 0.16\end{aligned} \tag{16}$$

R_f can be derived by the function of bulk Richardson number, R_i at each grid point (KIMURA, 1983; MELLOR and YAMADA, 1974; YAMADA and MELLOR, 1973) as

$$\begin{aligned}R_f &= 0.6588\{R_1 + 0.1776 - (R_1^2 - 0.3221 R_1 \\ &\quad + 0.03156)^{1/2}\} \qquad \text{for } R_i \leq 0.19 \\ R_i &= g/\Theta.\ \Delta\theta.\ \Delta z/\Delta U^2\end{aligned} \tag{17}$$

From the balance between production of turbulent energy due to both shear and buoancy and dissipation of turbulent energy, turbulent velocity, $e = (e^2)^{1/2}$ can be evaluated by

$$\begin{aligned}e^2 &= B_1 \ell^2 \{S_m(z_T/h)^2\ \{(\partial_z u)^2 + (\partial_z v)^2\} \\ &\quad - g/\Theta S_h(z_T/h)\partial_z \theta\} \\ B_1 &= 16.6\end{aligned} \tag{18}$$

c. Radiation process

Long wave radiations are absorbed by water vapor and carbon dioxide in the lower atmosphere. Considering that flux from the ground surface toward the upper levels is regarded as positive, total net flux of long wave radiation, R_g yields to

$$\begin{aligned} R_g &= \sigma T_c^4 \tau_c + \sigma (T_{oo}^4 - T_c^4) \tau_f(U_{oo}) \\ &\quad + \Sigma \sigma (T_1^4 - T_{1+1}^4) \tau_f(|U_i|) \\ T_c &= 220\mathrm{K} \end{aligned} \tag{19}$$

In the above, σ is Stefan-Boltzman's constant, and T_c, T_{00} and T_i are critical temperature, temperature at the top of model atmosphere and temperature at the i-th level, respectively. Here, transmission function, τ_f is derived as follows :

$$\begin{aligned} \tau_f &= \tau_{H2O} \cdot \tau_{CO2} \\ \tau_{H2O} &= (1 + 1.746 U_*^{0.423})^{-1} \\ \tau_{CO2} &= 0.93 - 0.066 LOG_{10}(U_{*CO2}) \\ \tau_c &= (1 + 3.0 U_*^{0.408})^{-1} \tau_{CO2} \\ U_* &= 1/g \int q (p/p_0)^{0.6} dp \\ U_{*CO2} &= (p_0^2 - p^2)/p_0^2 \end{aligned} \tag{20}$$

where τ_{H2O}, τ_{CO2} and τ_c are the transmission functions for H_2O, CO_2 and critical temperature (=220K). U_*, q, p_0 and p are effective vapour amount, specific humidity (g/cm^2), pressure (mb) at the surface and at the arbitary levels.

In this model, considering the absorption of solar radiation by water vapor due to Rayleigh scattering and the solar radiation toward the earth surface as a positive flux, total net solar radiation at the ground is given by

$$\begin{aligned} S_g &= (1 - \alpha_S) \{ S_{OS}(1 - \alpha_A)/(1 - \alpha_A \alpha_S) \\ &\quad + S_{OA}(1 - A(x)) \} \\ S_{OS} &= 0.651\, S_O \cos\zeta \\ S_{OA} &= 0.349\, S_O \cos\zeta \end{aligned} \tag{21}$$

and

$$\begin{aligned} \cos\zeta &= \cos\phi \cos\delta \cos h + \sin\phi \sin\delta \\ \alpha_A &= 0.085 - 0.247 LOG_{10}(p/p_0 \sec\zeta) \\ A(x) &= 0.273 x^{0.303} \\ x &= U_{*T} \sec\zeta \end{aligned} \tag{22}$$

where S_O, S_{OS} and S_{OA} are solar constant, scattering part of solar radiation (wave length; $\lambda < 0.9\mu$) and absorption one ($\lambda > 0.9\mu$). ζ is solar zenth angle, which is a function of latitude(ϕ), declination(δ) and time angle(h). $A(x)$ is an absorbing function of solar radiation, and α_S and α_A are albedos of atmosphere and earth surface, respectively.

Q_r, which is the heating rate of atmosphere can be approximated by the following Newtonian cooling due to long wave radiation as

$$Q_r = 10^{-5}(T_g - T) \quad \text{for } T > T_g \tag{23}$$

$$Q_r = 0 \quad \text{for } T \le T_g \tag{24}$$

where T and T_g are air temperature and soil temperature at the ground level.

d. Similarity theory in the surface layer

Assuming that the lowest level of the model set at 10m in the surfece layer is a constant flux layer and similarity theory can be applied to parameterize vertical turbulence. Considering energy balance near the surface momentum flux, τ, sensible heat flux H and latent heat flux, E are

$$\begin{aligned} \tau/\rho &= -(u_*)^2 = -k^2 u^2/\phi_m^2 \\ H/(C_p \rho) &= -\theta_* u_* = -k^2 |u| (\theta_1 - \theta_g)/(\phi_m \phi_h) \\ E/(L\rho) &= -q_* u_* = -k^2 |u| (q_1 - q_g)/(\phi_m \phi_h) \end{aligned} \tag{25}$$

ρ, q_*, u_* and k are the air density, the water vapor scale, friction velocity, θ_* the potential temperature scale and the Von Karman constant. The subscription 1 and g mean the lowest and ground level of the model domain.

BUSINGER (1973), HSU (1988), MONIN (1970), PANOFSKY and DUTTON (1984), PAULSON (1970) and WILLIAMS (1980) describe various kinds of formulae on the integrated universal functions, ϕ_m for momentum and ϕ_h for heat and we use the following formula suggested by KIMURA and TAKAHASHI (1991)

$$\begin{aligned} \phi_m &= \int \Phi_m/\zeta \, d\zeta \\ \phi_h &= \int \Phi_h/\zeta \, d\zeta \end{aligned} \tag{26}$$

here $\zeta = z/L$, $\zeta_0 = z_0 L$ and L is Monin-Obukhov length scale defined as

$$L = \rho C_p \theta u_*^3/kgH \tag{27}$$

Under unstable condition

$$\begin{aligned} \Phi_m &= (1 - 16\zeta)^{-1/4} \\ \Phi_h &= (1 - 16\zeta)^{-1/2} \quad \text{for } \zeta \le 0 \end{aligned} \tag{28}$$

Under stable condition, two classifications for momentum and heat are given by

$$\Phi_m = 1 + 7\zeta$$

$$\Phi_h = 1 + 7\zeta \qquad \text{for } 0 < \zeta \leq \zeta_0 \tag{29}$$

and

$$\Phi_m = 1 + 7\zeta_0$$
$$\Phi_h = 1 + 7\zeta_0 \qquad \text{for } \zeta_0 < \zeta \tag{30}$$

where

$$\zeta_0 = z_0/L = 0.714$$
$$\zeta = R_i \phi_m^2 / \phi_h \tag{31}$$
$$R_i = g/\Theta(\theta_1 - \theta_g)\Delta z_1/|u|^2$$

For the prediction of earth surface temperature in the case of bare ground condition, a force restore method suggested by Deardorff (1978) are derived as

$$\partial t\, \theta_g = (S_g - R_g - H - E)/C_1 - (\theta_g - \theta_0)/C_2 \tag{32}$$

where θ_g and θ_0 are ground surface potential temperature and underground temperature. C_1 and C_2 can be evaluated by diurnal period, τ_d ($=24^h$), heat capacity of underground soil, C_g (cal/cm^3/K) and heat conductivity, k_g(cal/cm/k/sec) as

$$C_1 = 0.5(\tau_d C_g K_g / 2\pi)^{1/2}$$
$$C_2 = \tau_d / 2\pi \tag{33}$$

and π is pi.

If evaporation coefficient, B_g at the ground is treated as constant, specific humidity at the ground surface, q_g yields to

$$q_g = B_g\, q_s(T_g) + (1 - B_g) q_1 \qquad \text{for } q_s(T_g) \geq q_1$$
$$q_g = q_s(T_g) \qquad \text{for } q_s(T_g) < q_1 \tag{34}$$

wetness of bare ground, w_g($=0.2$cal/cm^3/k), which is defined as the ratio of available water content to maximum available water content has different value depending upon season. In this study w_g is treated as 0.2 for the spring time as CHOI and CHOI (1995) and can be predicted as

$$C_g = 0.2(1 + w_g)$$
$$k_g = (0.386 + 0.15 w_g)10^{-2} \tag{35}$$
$$B_g = \min(1, 2w_g)$$

4. Result of numerical simulation

a. Horizontal surface winds

The model forecasting of the wind in the mountainous coastal region is of primary interest in explaining atmospheric circulations over the eastern coastal seas of Korea. In the case of prevailing strong synoptic scale westerly winds blowing over the north-eastern Asian counties such as China, Korea and Japan from March 26 through 28, 1994. we three-dimensionally simulated coastal wind fields by using a non-hydrostatic numerical model. On March 26, that is, one day before carring out numerical simulation the surface winds were generally moderate and the wind fields had typical wind patterns like sea and land breeze in the Kangnung coastal region.

At 12 LST on March 27, 1994 strong westerly winds penetrate into Korean peninsula and pass by eastern coastal mountain regions (Fig. 1). At the same time strongly enforced local winds are detected near Kangnung coastal regions (Fig. 3-a). In Fig. 3a the surface winds at 12 LST, March 27, 1994 in the eastern mountainous coastal region of Kangnung city, adjacent to East Sea (The Sea of Japan) consist of two different kinds of coastal winds such as synoptic scale westerly and meso scale easterly. Along the coastal line, which lies from south to north-west, strong westerly winds with a speed more than 18m/s blow over the inland high mountains (Mt. Taegwallyang) toward East Sea, but easterly winds with a speed of 7m/s in the coastal sea also approach to inland of the coast. Since these two different kinds of winds in the opposite directions are in the confront each other, and the surface winds at 10m height are very weak, especially 2m/s near the surface at the edge of lee side of Taegwallyang mountain, but the surface wind speeds with easterly in the Kangnung city are in the range of 3m/s to 5m/s. These westerly winds were modified from orginal synoptic scale winds, which were enforced by flowing over the large steep mountains (Mt. Taegwallyang or Mt. Whangbang) like a wind storm. On the other hands, the easterly winds are caused by a sea-breeze due to the meso-scale thermal forcing from the difference between the air temperature over the ground and that over the sea surface in the daytime.

At 15 LST, as daytime goes on, the sea breeze was more intensified and the easterly wind

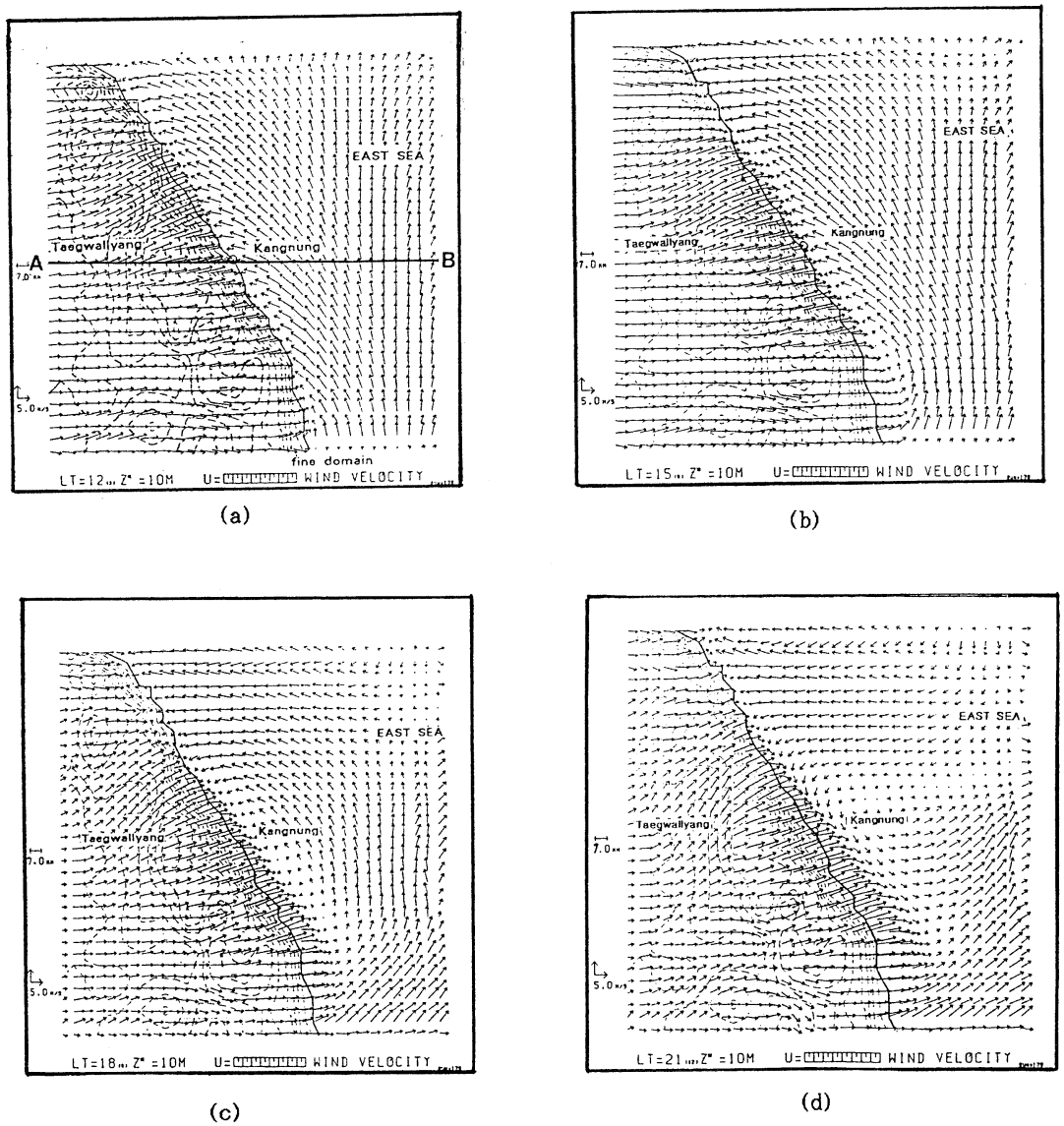

Fig. 3. Suface winds (m/s) at 10m height over topography near Kangnung coastal regions of Korea (——means coast line) at 12 (a), 15 (b), 18 (c) and 21 (d) LST, March 27, 1994.

speeds became slightly higher than that of 12 LST (Fig. 3b). At the same time, as the synoptic scale inland westerly winds in front of the mountains became stronger and stronger, they could be downslope wind storms along the eastern slope of the mountains. Under this situation the surface winds in the Kangnung area between lee side of the mountain and coastal sea became weaker and weaker, and reached to 2m/s.

Similar to 15 LST, the sea breeze cycle at 18 LST, just before sunset became smaller and shallower, and the surface wind patterns still show easterly with the more wide area of weak winds over the coastal sea surface in offshore sides of Kangnung city (Fig. 3-c). This feature is attributed to the intrusion of more intensified westerly winds toward the coastal sea, as the sea breeze was weaken with a shortage of solar radiation. In the simulation, a zone of the

minimum wind speed appears near the shoreline.

After sunset such as 21 and 00 LST, there was no sea breeze near the coast and the meso-scale forcing in the opposite direction due to surface cooling of ground could induce a land breeze from inland toward sea (Fig. 3-d, 4-a). The existed westerly winds in the inland sides was associated with the land breeze and could be more intensified with a higher speed at night. Especially, from 03 through 09 LST, March 28, strong weaterly surface winds with speeds of 18m/s can stretch out to 200km off coast and from those points to open sea sides, the westerly surface winds could not be affected by orographic features. So the surface winds near Kangnung were not over the limit of 5m/s.

In the present work, a localized wind generated a circulation was detected with width of 110km (east-west) and 80km (north-south) in the coastal sea near Kangnung and rotated in an cyclonic direction (counter-clockwise). These circulations over the coastal sea surface, which tend to be smaller and smaller, exist until next day morning 09 LST (Fig. 4-b, 4-c, 4-d). These localized wind circulations over the sea surface may considerably affect formations of coastal oceanic circulations.

At 09 LST the surface winds continue to be eastward over both inland and sea surfaces. In the lee-side of mountains the strong downslope wind storms continuously prevail throghout the coastal region and the extension of localized westerly winds remains in the coastal sea (Fig. 4-d). In the open sea, the relatively weak surface winds induced by land breeze have the same eastward direction, because the surface cooling on the inland ground continues to exist. After 09 LST the surface wind pattern becomes similar to 12 LST, March 27. On March 29 the winds near Kangnung mountainous coastal region become moderate again with the similar structure of wind on March 26.

b. Vertical profiles of winds

Vertical profiles of wind vectors with speed and direction on 15 levels over the east-west straight cutting line from Kangnung (east) to Mt. Taegwallyang (west) (A−B line in Fig. 3-a) in the fine-mesh model domain (Fig. 5∼Fig. 8). As the synoptic scale westerly winds in the eastern coastal region rapidly flow over the large steep mountains, they can be localized to be strong downslope winds and changed to be internal gravity waves generated in the lee-side of mountain and over coastal seas. Hence, from the vertical profiles of horizontal wind speed at each level of 15 levels, the downslope winds get hydraulic jump motions with bounding forward, and the enhancement of downslope winds could produce wind storms along the east slope of the mountain, which move toward the eastern coastal sea (Fig. 2).

At 12 and LST, March 27 during the daytime a sea breeze circulation takes a place from sea toward inland sites, but the sea breeze circulation can stretch out to just coastal site due to the eastward propagation of internal gravity waves (Fig. 5a and 5b). It is not easy to find an upslope wind in the eastern side of coastal mountains, which can be often observed under the easterly synoptic wind or meso-scale sea breeze. It means that the sea breeze could not penetrate into the top of the mountain and be limited to the inland coast. As the westerly downslope winds confront the easterly sea breeze in Kangnung city, the some amount of air should be isolated, but the others move upward, blowing toward the sea side. Thus, the surface winds at inland coastal sites were relatively weaker than those in the open sea or the further inland sites from the coast.

Through the our numerical simulation, two different kinds of atmospheric circulations (two eddies) in the lee side of the mountain were detected such as an internal gravity wave circulation with westerly wind and a sea breeze circulation with both easterly wind near the sea surface and westerly in the upper level such as a circular flow pattern (Fig. 7a and 7b). Under the existance of two kinds of atmospheric circulations, the air near Kangnung coastal region should be trapped by the two circulations in the opposite directions, and the horizontal surface wind speed of the downslope wind near coast should be reduced to be about 2.0 m/s, that is, relatively weak by the intrusion of sea breeze. Fig. 7a and 7b show that as the westerly wind storms can drive out

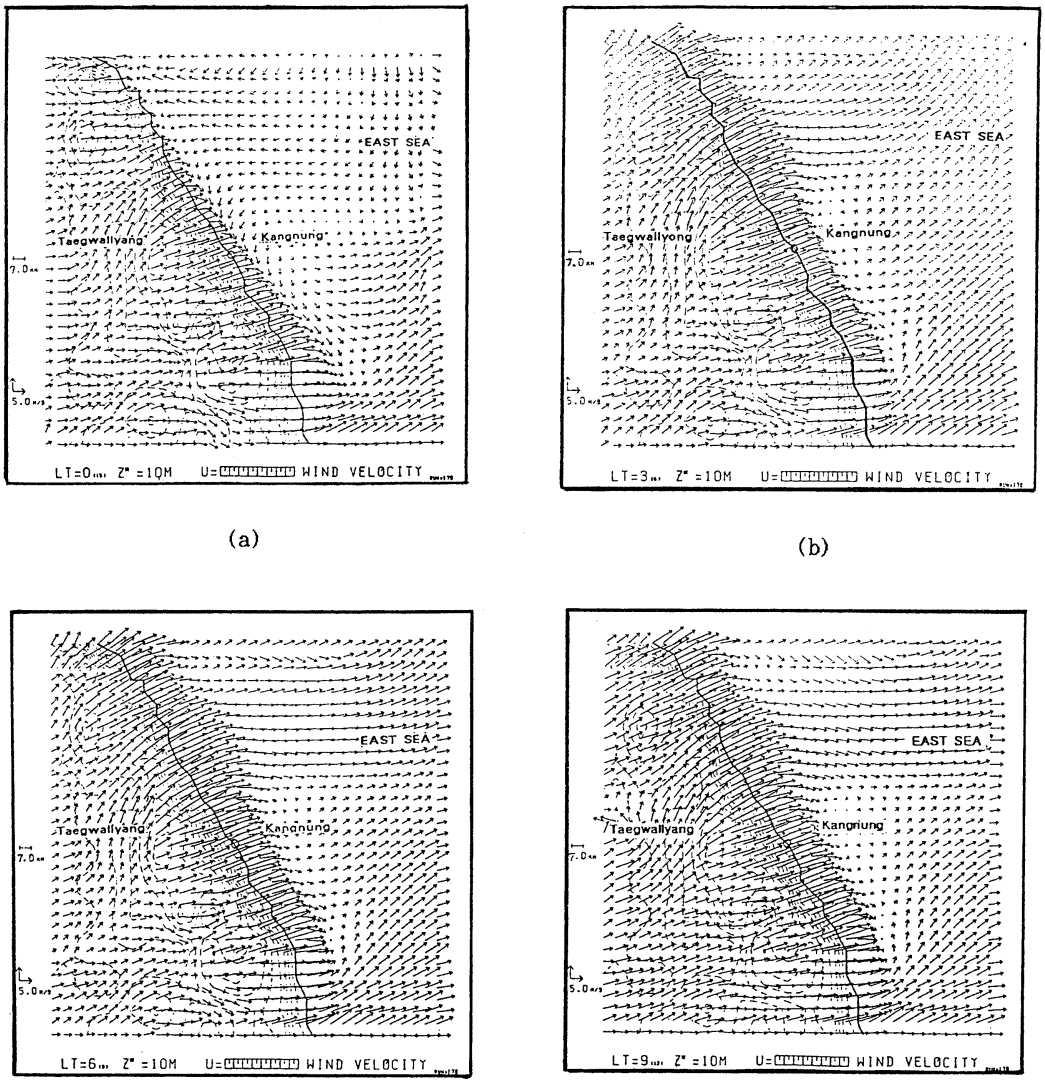

Fig. 4. As shown in Fig. 3 expect for 00 (a), 03 (b), 06 (c) and 09 (d) LST March 28, 1994.

the meso scale easterly winds such as sea breeze to the coast, the positions of minimum wind speed lie in lower and lower levels along the eastern slope of the mountain and eventually moves to the coastal sea. Of course, the wind at Kangnung city are easterly with 3 m/s under the influence of the sea breeze circulation.

At 18 LST, near sunset the wind pattern was similar to that at both 12 LST and 15 LST, but the depth of the sea breeze circulation became shallower and shallower with weak wind speeds (Fig. 5c, 7c). As the nighttime went on, that is, from 21 LST, March 27 through 06 LST, March 28, the vertical convection of air from the earth surface should be suppressed due to the disappearance of solar radiation, and then, the momentum could be transported from the strong upper level winds toward the surface, enhancing the existed daytime downslope

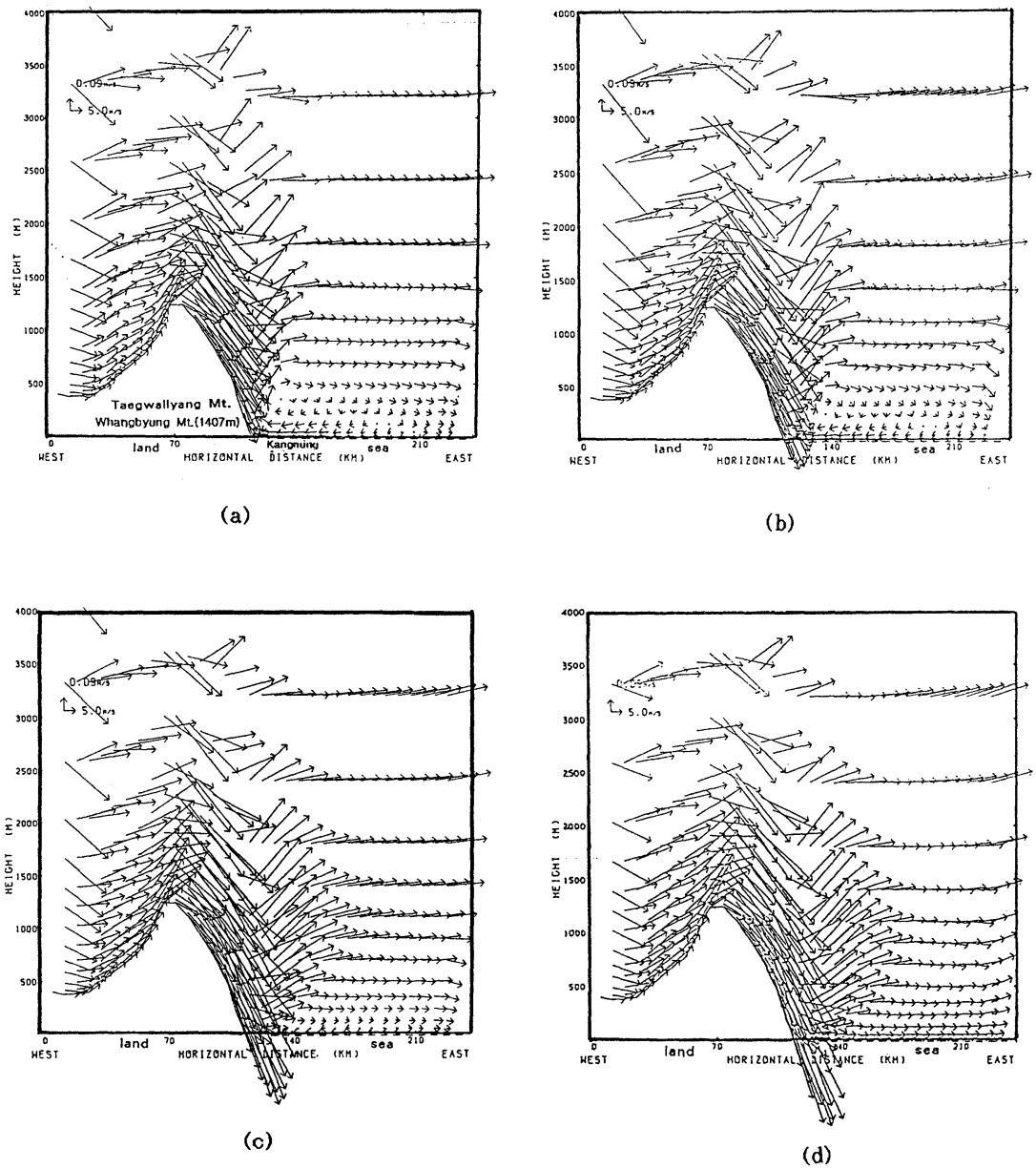

Fig. 5. Vertical profiles of wind vectors (m/s) on 15 levels over the east-west straight cutting line from Kangnung near to Mt. Taegwallyang (A-B line in Fig. 3a) at 12 (a), 15 (b), 18 (c) and 21 (d) LST, March 27, 1994.

wind storms to be more intensified at night than in the daytime (Fig. 5d, 6a, 6b). As mentioned above, in Fig. 7d, 8a, 8b and 8c the centers of wind storms with maximum wind speeds over 28m/s take positions lower and lower toward the ground surface and come down to the height of 200m over the ground at 06 LST just before sunrise.

Furthermore, during the night the air over the inland surface was much cooler than that over sea surface, due to the cooling of ground surface and then, the meso-scale temperature

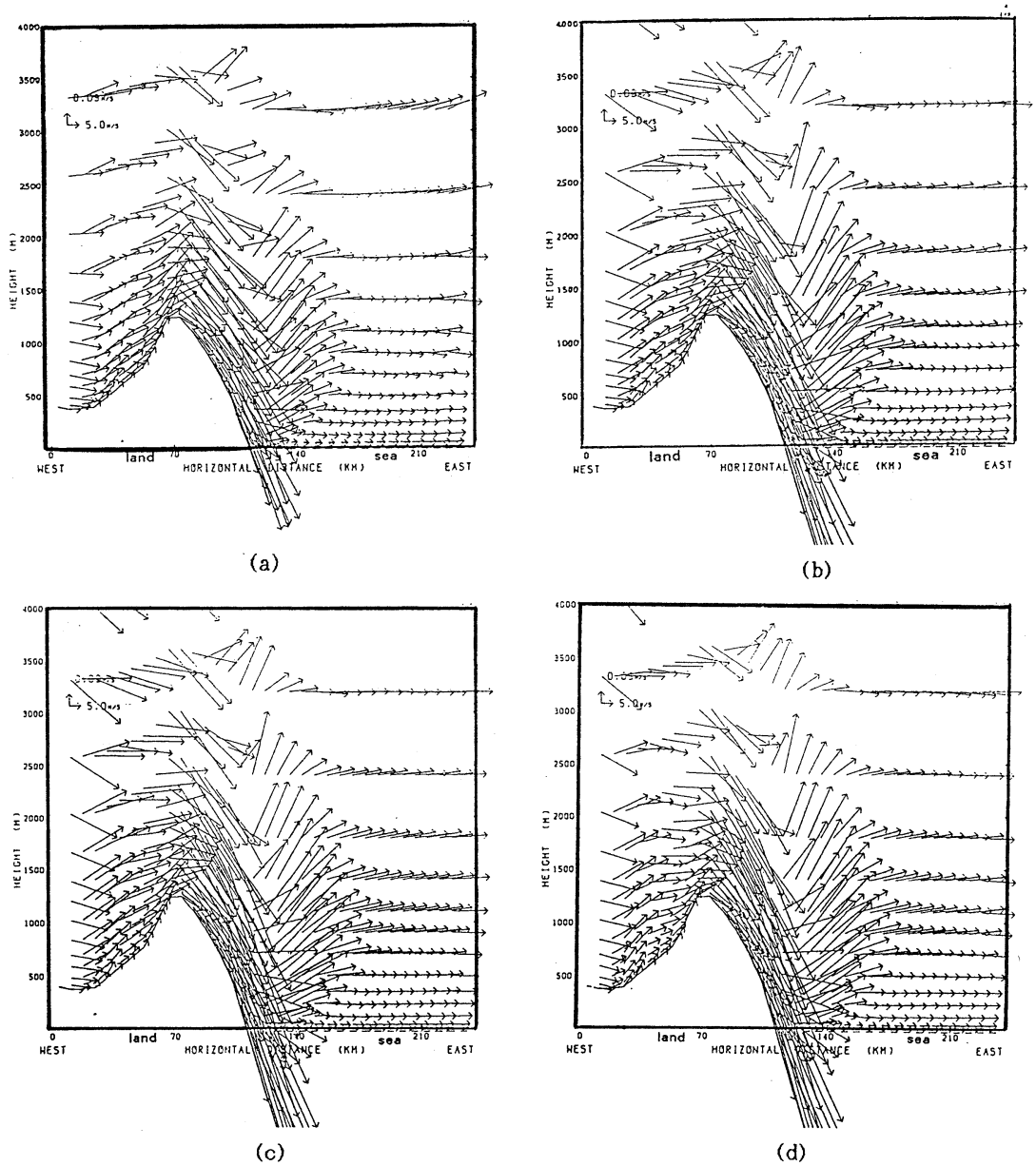

Fig. 6. As shown in Fig. 5 expect for 00 (a), 03 (b), 06 (c) and 09 (d) LST March 28, 1994.

contrast between air over the ground and that over the sea surface occurs, resulting in generating a land breeze from inland toward sea. Thus, the surface winds near the Kangnung city became strong. So, since the westerly downslope wind storms intensified by both orographic feature with a sharp inclination and momentum transfer from the strong upper level winds toward the ground surface, after sunset, can be associated with the land breeze blowing from inland toward sea, they produce one atmospheric circulation (one cell) in the coastal region and enhance the surface winds near the Kangnung city to be stronger and stronger (7d and 8a).

At 06 lst on the next day morning, that is,

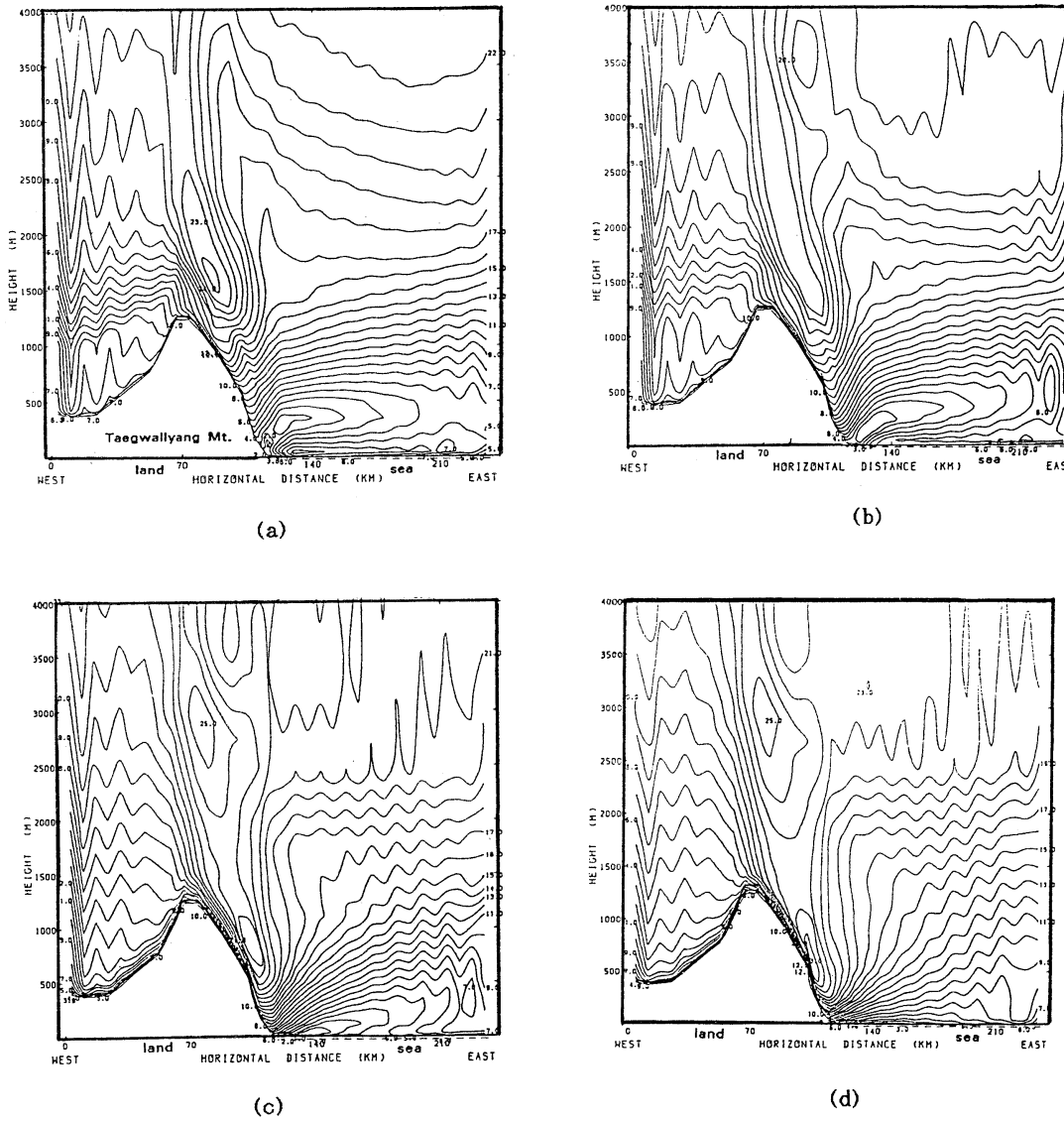

Fig. 7. Vertical profiles of horizontal wind speeds (m/s) on 15 levels over the east-west straight cutting line from Kangnung near to Taegwallyang Mt. (A-B line in Fig. 3a) at 12 (a), 15 (b), 18 (c) and 21 (d) LST, March 27, 1994.

sunrise time, as the center of the wind storm was located in the lowest level near the surface, due to both maximum momentum transfer from the upper layer and maximum effect of land breeze, the surface winds induced by the strong downslope wind storms were still westerly. Because it takes more time to excite air by solar radiation and sea breeze can just start to be generated at this time (Fig. 6c and 8c). The center of the wind storm at 09 LST was located at the slightly heigher position than at 06 LST, as the sea breeze started, and the strong westerly winds could suppress the easterly sea breeze, showing the resultant westerly surface winds near Kangnung city (Fig. 6d and 8d).

During the day, on March 28, the wind patterns were very similar to those on March 27. After 09 LST March 28, especially under the

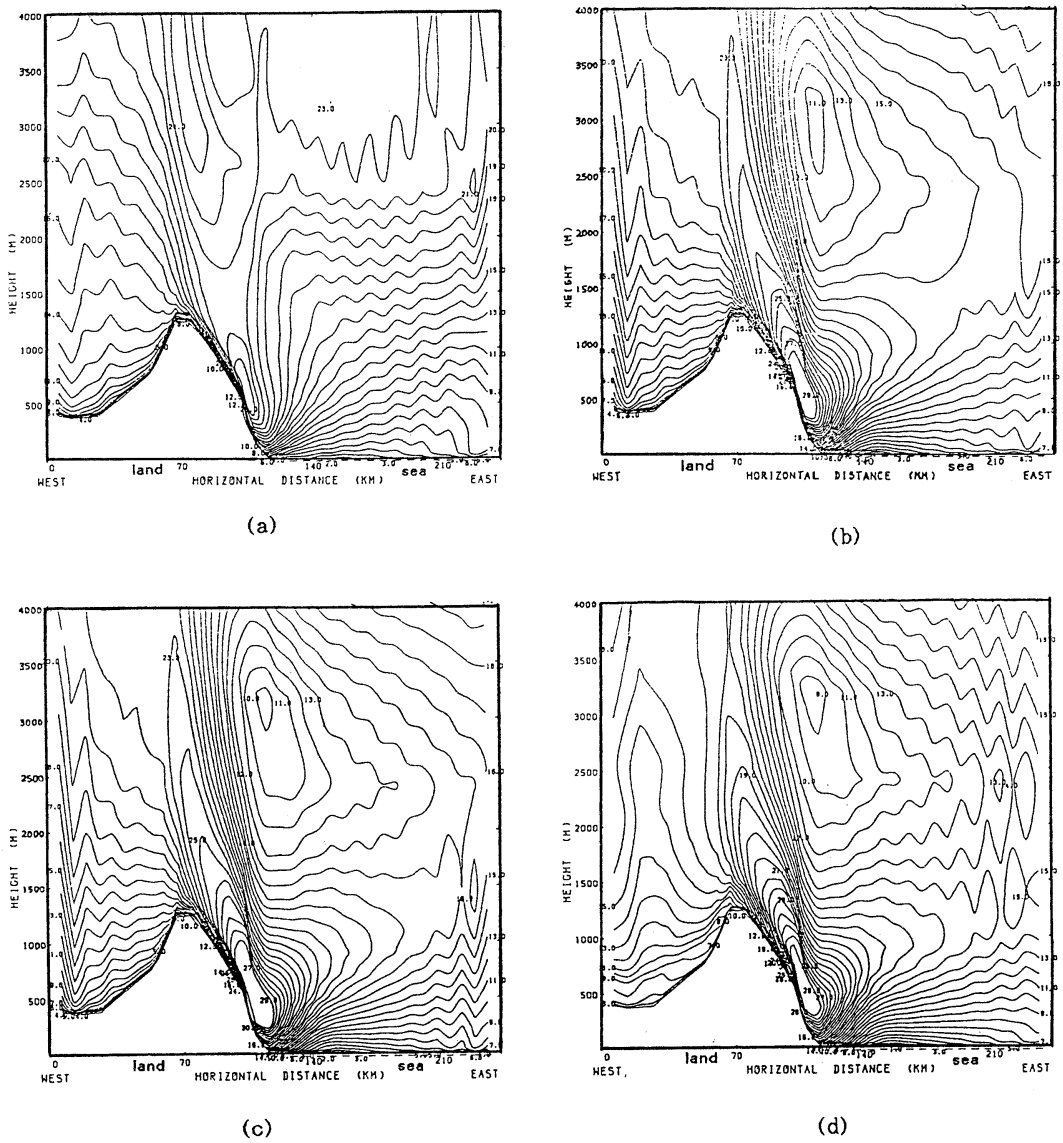

Fig. 8. As shown in Fig. 7 expect for 00 (a), 03 (b), 06 (c) and 09 (d) LST March 28, 1994.

strong development of downslope wind storms along the east slope of the mountain and in the lower layer over the coastal region, two kinds of circulations induced by both internal gravity waves and sea breeze should be produced again at Kangnung city and the surface wind speed was 18 m/s. The wind patterns in the coastal region on March 28 was similiar to the previous daytime case. On March 29, the winds became moderate again and a typical wind pattern controlled by only sea-land breeze was observed in the coastal region of Kangnung.

c. Comparision of simulated winds to measured ones

Under the severe downslope wind storms in the mountainous coastal region of Kangnung, the comparision of simulated winds to the observed one was made by using a pival balloon launched from Korean Air Force Base of

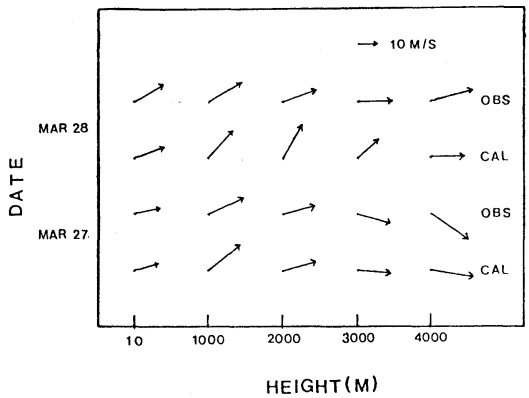

Fig. 9. Comparision of calculated wind vectors with observed ones at Korean Air Force Base of Kangnung from March 27 through March 28, 1994.

Kangnung city at 09 LST, every day from March 27 through 29, 1994. The measured height were 10m, 1000m, 2000m, 3000m and 4000m (Fig. 9). On March 27, the simulated wind speed and directions (measured wind speed and directions) at 10m height over the ground of Kangnung Air Force Base was 13m /s, 255° (14m/s, 260°) at 10m, 22.5m/s, 230° (21 m/s, 245°) at 1000m ; 18m/s, 256°(18m/s, 255°) at 2000m, 18m/s, 275° (18m/s, 285°) at 3000m and 24.1m/s, 278° (24m/s, 305°) at 4000m, respectively. At 09 LST on the next day morning, March 28, they are 17.5m/s, 250° (18m/s, 240°) at 10m, 20m/s, 225° (21m/s, 240°) at 1000m, 20m/s, 220° (19m/s, 250°) at 2000m, 15.6m/s, 230° (19 m/s, 270°) at 3000m, 18.5m/s and 280° (24m/s, 265°) at 4000m under the existence of wind storms. Even if there were, in part, a little differences between the simulated winds and the observed ones, they well agreed each other. Thus, when the severe downslope wind storm and sea-land breeze occur over complex terrain near the coast, the numerical forecasting for atmospheric circulations can be expected to play a significant role in prediction of wind driven currents and wind waves on the mountainous coastal seas and it is very useful to operate a non-hydrostatic numerical model for the prediction of coastal sea states.

5. Summary

Numerical experiments of atmospheric circulations were performed under the downslope wind storms generated in the lee-side of mountainous coastal region. In the daytime we have two different kinds of atmospheric circulations, which consist of an internal gravity wave circulation with westerly wind and a sea breeze circulation with both easterly wind near the sea surface and westerly in the upper layer. The internal gravity waves toward sea and the sea breeze circulation toward inland caused an isolation of air at Kangnung coastal site. Thus, surface winds near the coastal seas were relatively weaker than those in the open sea or inland.

On the other hand, at night under the intensification of westerly downslope wind storms associated with land breeze toward sea and the momentum transfer from the upeer level toward the coastal surface, the surface winds became much stronger at night than during the day in the coastal region. Consequently, when the downslope wind storms were strongly developed, the surface wind speeds at Kangnung city also became higher and it might excite the severe sea states in the coastal regions.

Acknowledgements

For the successful execution of this coastal experiment, the author would like to express much thanks to Mr. S. TAKAHASHI, Dr. T. Y OSHIKAWA and Dr. T. HANAFUSA of Meteorological Research Institute, Japan Meteorological Agency for using computer facility and technical assistance with helpful discussions. He is also grateful for oceangraphical data provided by Korea Oceanographic Data Center, National Fisheries Research and Development Agency. This paper was supported in part by NON DIRECTED RESEARCH FUND, Korea Research Foundation, Ministry of Education in 1995, under grant for "Variation of atmospheric pollution concentrations due to the development of internal gravity waves in Kangwondo coastal regions". Another financial aid was provided by Ministry of Environment and Ministry of Science & Technology in 1995 for "Regional climate modelling-research and development on technology for global environmental monitoring and change prediction".

References

BOER, G. J., N. A. MCFARLANE and R. LAPRISE, (1984) : The climatology of Canadian climate center general circulation model as obtained from a five-year simulation. Atmos. Ocean, **22**, 430–473.

BUSINGER, J. A. (1973) : Turbulence transfer in the atmospheric surface layer, *In* Workshop on Micrometeorology, Haugen, D. A. (ed). Amer. Meteor. Soc., 67～100.

CHOI, H. and J. CHOI (1994) : Characteristics of onshore winds in the coastal thermal internal boundary layer. J. Korean Meteor. Soc., **30**, 1～11.

CHOI, H. and J. CHOI (1995) : Atmospheric pollutant concentrations under the influence of internal gravity wave and sea-land breeze circulations in the mountainous coastal regions. Korean J. Geophys. Res., **23**, 18–33.

CHOI, H., J. CHOI, S. TAKAHASHI and T. YOSHIKAWA (1996) : Three dimensional numerical modelling on the growth of coastal thermal internal boundary layers in the Cheju island of Korea. J. Korean Meteor. Soc., **32**, 1–16.

DAVIS, H. C. (1987) : Observational studies and interpretation of the mountain pressure drag during ALPEX, in observation, theory and modelling of orographic effects, ECMWF. Reading. **113**, 136pp.

DURRAN, D. R. and J. B. KLEMP (1987) : Another look at downslope wind storms, Part II : Non linear aplication beneath wave overturning layers. J. Atmos. Sci, **44**, 3402–3412.

DEARDOFF, J. W. (1978) : Efficient prediction of ground surface temperature and moisture with inclusion of a layer of vegetation. J. Geophys. Res., **38**, 659–661.

FRIEHE, C. A. and C. D. WINANT (1982) : Observation of wind and sea surface temperature structure off of the northern California coast. 1st International Conference on Meteorology and Air/Sea Interaction of the Coastal Zone, Hague, Amer. Meteor. Soc., 209–214.

HSU, S. A. (1980) : Research in the coastal meteorology : basic and applied. 2nd Conference on Coastal Meteorology, Los Angles, Amer. Meteor. Soc., 1–7.

HSU, S.A. (1988) : Coastal Meteorology. Academic Press. 260pp.

KIMURA, F. (1983) : A numerical simulation of local winds and photochemical air pollution (I) : two dimensional land and sea breeze. J. Meteor. Soc. Japan, **61**, 862–878.

KIMURA, F. and S. TAKAHASHI (1991) : The effects of land-use and anthropogenic heating on the surface temperature in the Tokyo metropolitan area : numerical experiment. Atmos. Environ., **25**, 155–164.

KLEMP, J. B. and D. R. DURRAN (1983) : An upper condition permitting internal gravity wave radiation in numerical mesoscale models. Mon. Wea. Rev. **111**, 430–440.

LANGLAND, R. H., P. M., TAG and R. W. FETT (1987) : Numerical simulation of a satellite-observed calm zone in Monterey Bay, California. Mon. Wea. Rev., **2**, 261–268.

LEE, Y. (1982) : The prediction of thermal internal boundary layer growth and fumigation. 1st International Conference on Meteorology and Air / Sea Interaction of the Coastal Zone, Hague, Amer. Meteor. Soc., 83–86.

LILLY, D. K, J. M. NICHOLLS, R. M. CHERVIN, P. J. K ENNEDY and J. B. KLEMP (1982) : Aircraft measurements of wave momentum flux over the Colorado Rocky mountains. Q. J. R. Meteor. Soc., **108**, 625–642.

MCPHERSON, R. D. (1970) : A numerical study of the effect of a coastal irregularity on the sea breeze. J. of App. Meteor., **9**, 767–777.

MELLOR, G. L. and T. YAMADA (1974) : A hierachy of turbulence closure models of planetary boundary layers. J. Atmos. Sci., **31**, 1791–1805.

MONIN, A. S. (1970) : The atmospheric boundary layer. Annual Review of Fluid Mechanics, **2**, 225–250.

NFRDA. (1994) : Analyzed NOAA satellite pictures on the sea surface temepratures in the East Sea (Japan Sea). National Fisheries Research and Development Agency.

ORLANSKI, I. (1976) : A simple boundary condition for unbounded hyperbolic flows. J. Comp. Phys., **21**, 251–269.

PALMER, T. N., G. J. SMITH and R. SWINBANK (1986) : Alleviation of a systematic westerly bias in general circulation and NWP models for trough and orographic gravity wave drag parameterization Q. J. R. Meteor. Soc., **112**, 1001–1039.

PANOFSKY, H. A. and J. A. DUTTON (1984) : Atmospheric Turbulence. John & Wiley, New York, 1–100.

PAULSON, C. A. (1970) : The mathematical representation of wind speed and temperature profiles in the unstable atmospheric surface layer. J. App. Meteor., **9**, 857–861.

PELTIER, W. R. and T. L. CLARK (1979) : The evolution and stability of finite amplitude mountain waves. Part II : Surface wave drag and severe downslope windstorms. J. Atmos. Sci., **36**, 1498–1529.

PLATE, E. J. (1971) : Aerodynamic characteristics of atmospheric boundary layers. U. S. Atmospheric Energy Commission, 190pp.

RAYNOR, G. S., S. SETHURAMAN and R. M. BROWN (1979) : Formation and characteristics of coastal

internal boundary layer during onshore flows. Boundary Layer Meteor., **16**, 487–514.

ROLL, H. V. (1965) : Physics of the marine atmosphere. Academic press, New York, 426pp.

SATOMURA, T. and P. BOUGEAULT (1992) : Orographic wave drag during PYREX experiment. *In* Spring Meeting of the Meteorological Society of Japan, Tsukuba, 282pp.

SEGAL, M., R. T. MCNIDER, R. A. PIELKE and D. S. MCDOUGAL (1982) : A numerical model simulation of the regional air pollution meteorology of the greater Chesapeake Bay area–summer day case study. Atmos. Environ., **16**, 1381–1397.

SETHURAMAN, S. (1982) : Observation of the bounadry layer wind structure near land–sea interface. 1st International Conference on Meteorology and Air/Sea Interaction of the Coastal Zone, Hague, Amer. Meteor. Soc., 4–7.

SMITH, R. B. (1978) : A measurement of mountain drag. J. Atmos. Sci., **35**, 1644–1654.

SMITH, R. B. (1989) : Hydrostatic airflow over mountains. Adv. Geophys., **31**, 1–41.

SMOLARKIEWICZ, P. K. and R. ROTUNNO (1989) : Low Froude number flow past three dimensional obstacles. Part I : Baroclinically generated lee vorties. J. Atmos. Sci., **46**, 1154–1164.

WILLIARMS, R. G. (1980) : A procedure for wind field construction from measured data which utilizes local surface roughness. 2nd Corference on Coastal Meteorology, Los Angles, Amer. Meteor. Soc., 307pp.

WMO. (1986) : Scientific results of the Alpine experiment. GARP pubilication series, 27, WMO, Geneva.

YAMADA, T. (1983) : Simulation of nocturnal drainage flows by a q^2–1 turbulence closure model. J. Atmos. Sci., **40**, 91–106.

YAMADA, T. and G. L. MELLOR (1973) : A numerical simulation of the BOMEX data using a turbulence closure model coupled with ensemble cloud relations. Q. J. R. Meteor. Soc., **105**, 95–944.

Received January 4, 1996
Accepted March 18, 1996